BULLETIN OF THE CHEMICAL SOCIETY OF JAPAN, VOL. 45, 401—407 (1972)

Spin Relaxation Effects on the ESR Spectrum of Gaseous Oxygen Atoms

Mamoru JINGUJI, Yuji MORI, and Ikuzo TANAKA

Department of Chemistry, Tokyo Institute of Technology, Ohokayama, Meguro-ku, Tokyo

(Received July 7, 1971)

The linewidths of the single-quantum transitions of $O(^3P_1)$ and $O(^3P_2)$ in gaseous diluents, such as oxygen molecules and an inter gas, are measured with an ESR spectrometer of a usual type. The cross sections calculated from the pressure broadening are given. With regard to the multiple-quantum transitions in the Zeeman sublevels of $O(^3P_2)$, the dependence of the linewidths on the pressure is duscussed. The spin-lattice relaxation time, T_1, for the single-quantum transitions of $O(^3P_1)$ or $O(^3P_2)$ is evaluated by employing the standard power saturation technique, and the effectiveness of an inert gas on T_1 is studied. The spin-lattice relaxation between the Zeeman sublevels of the O atom is caused by the coupling between the orbital momentum and the electron-spin state upon collision. With regard to the multiple-quantum, the relaxation mechanism is also studied. Finally, we study the relationship between the spin-lattice relaxation time, T_1, and the corresponding probabilities of $\Delta M_J = \pm 1$, $\Delta M_J = \pm 2$, $\Delta M_J = \pm 3$, and $\Delta M_J = \pm 4$ transition induced by collisions.

Recently studies of spin-relaxation phenomena in the gas phase with two different experimental techniques of ESR spectroscopy have been reported for S-state atoms. One is the measurement of the spin-lattice relaxation time, T_1, for the N atom by Brown and Brennen.[1] They noticed that the N atoms in the N_2 diluent have a long spin-lattice relaxation time and interpreted their data in terms of a lack of equilibration in the portion of the flow tube in the external magnetic field up to the cavity. On the other hand, Westenberg and deHaas[2] have obtained T_1 for the H atom by employing the standard power saturation technique; they have found that O_2 is effective in shortening T_1. We have now investigated the spin relaxation phenomena between Zeeman sublevels of O atoms. It is well known that the ground state of the O atom is ^3P, which is split into three states, $^3P_0$, $^3P_1$, and $^3P_2$, by the spin-orbit interaction. We observed the two absorption lines of the $^3P_1$ state and the four lines of the $^3P_2$ state at a low microwave power level and at a low pressure with the usual ESR technique. At lower pressures, we observed the spectra of the multiple-quantum transitions[3] at the expected position for the $^3P_2$ state with a higher microwave power.

In order to obtain the spin-lattice relaxation time for the single-quantum transition between Zeeman sublevels, we employed the standard power saturation technique formulated theoretically by Westenberg and deHaas.[2] This technique was extended to the measurement of T_1 in the multiple-quantum transitions. From the saturation studies of the four lines of the $^3P_2$ state, it was found that the relative absorption intensity of the two-quantum transition to the single-quantum transition is dependent on the pressure. A decrease in the pressure caused this relative intensity to change from a value of about 1/3 to a value of about 6. Since the spin-lattice relaxation in the gas phase is caused by the collision of the O atom with the oxygen molecule, these data show that the intensity of the multiple-quantum transi-

1) R. L. Brown and W. Brennen, *J. Chem. Phys.*, **47**, 4697 (1967).
2) A. A. Westenberg and N. deHaas, *ibid.*, **51**, 5215 (1969).
3) C. C. McDonald, *ibid.*, **39**, 3159 (1963).

tions is correlated with the spin relaxation phenomena. We measured the spin-lattice relaxation time for the single-, two-, and three-quantum transitions. An interpretation has been given of the dependence of T_1 on the pressure, and for the collisional relaxation mechanism in the gas phase. The analysis indicated that the values of T_1 for the single-, two-, and three-quantum transitions were of the order of 10^{-7}—10^{-6} sec in our system, and that, at any pressure, T_1 increased in this order. Then we investigated the variation in T_1 for the single-quantum transition of $O(^3P_2)$ in inert gas diluents, He, Ne, Ar, Kr, and Xe. The measurement of T_1 yielded the following cross sections for the spin-lattice relaxation: $\sigma_{O-He}=9.9$ Å^2, $\sigma_{O-Ne}=8.5$ Å^2, $\sigma_{O-Ar}=12$ Å^2, $\sigma_{O-Kr}=21$ Å^2, $\sigma_{O-Xe}=25$ Å^2, and $\sigma_{O-O_2}=33$ Å^2. It is concluded that the spin-lattice relaxation in O atoms is caused mainly by collisions between the O atom and inert gases through the strong spin-orbit coupling. Finally, we will discuss the relationship between the transition probabilities and the spin-lattice relaxation, using the experimental values of T_1 for the single-, two-, and three-quantum transitions.

Experimental

A JES-3BSX ESR spectrometer with a cylindrical TE_{011} mode cavity was used; the cavity frequency was about 9170 MHz. The magnetic field was modulated sinusoidally at a rate of 100 kHz, and the modulation amplitude was 28 mG. The loaded Q of the cavity was 2840. In order to obtain the spin-lattice relaxation time, the absolute value of microwave power was measured by a means of a thermister. The power (in gauss squared) of the microwave magnetic field, averaged over time and over the volume of the sample in the cavity, was estimated in the manner outlined by Poole.[4]

The flow of oxygen in the quartz tube, 10 mmϕ, was discharged in a cavity powered by a microwave generator (2450 MHz, 100 W) 50 cm upstream from the center of the ESR cavity. The measurements were carried out at total pressures from 0.02 to 0.3 Torr in order to obtain well-resolved spectra.

Theoretical

(i) The Single-quantum Transitions. Westenberg and deHaas[2] assumed that the homogeneous, unsaturated lineshape was Lorentzian, and they derived a general expression for the complex susceptibility in which the imaginary part represents the absorption of energy. Then, using Wahlquist's treatment,[5] they derived the following relation, which is convenient for saturation studies:

$$\left(\frac{H_1S_s}{H_{1R}S}\right)^{2/3}=\frac{0.53}{(2\mu^2T_1T_2/\hbar^2)^{1/3}H_{1R}{}^{2/3}}+0.53(2\mu^2T_1T_2/\hbar^2)^{2/3}H_{1R}{}^{4/3}\left(\frac{H_1{}^2}{H_{1R}{}^2}\right) \quad (1)$$

where μ^2 is the square of the absolute value of the transition matrix element in the direction of the microwave magnetic field, where $H_1{}^2$ is the average value of the microwave power in the sample, and where $H_{1R}{}^2$ is the absolute reference power of 1.54×10^{-4} G. S is the peak-to-peak amplitude, and S_s is the maximum value of S.

(ii) The Multiple-quantum Transitions. The theory of the multiple-quantum transitions was developed by Hughes and Geiger.[6] From their theory, we can expect that the intensities of the two- and three-quantum transitions will be proportional to the square and cube of the microwave power respectively. This relation is confirmed by the experimental results. There is experimental evidence that the lineshape of the two-quantum transition is adequately approximated by the Lorentzian lineshape, *i.e.*;

$$f(H-H_0)=\frac{\gamma T_2{}^*/\pi}{1+\gamma^2T_2{}^{*2}(H-H_0)^2},$$

where $T_2{}^*$ is a measure of the inverse observed linewidth. It is very closely connected with the area and the peak value of the lineshape. For the two-quantum transitions, we derived theoretically the following equation from the analogy of the single-quantum transitions, considering the dependence of the transition on the microwave power

$$\left(\frac{H_1{}^2S_s}{H_{1R}{}^2S}\right)^{2/3}=\frac{0.53}{(2\mu^2T_1T_2{}^*/\hbar^2)^{1/3}H_{1R}{}^{4/3}}+0.53(2\mu^2T_1T_2{}^*/\hbar^2)^{2/3}H_{1R}{}^{8/3}\left(\frac{H_1{}^2}{H_{1R}{}^2}\right)^2 \quad (2)$$

μ^2 in Eq. (2) is the square of the absolute value of the matrix element for the two-quantum transition, which is different from that of the single-quantum transition as given by Hughes and Geiger.[6] In the case of the three-quantum transitions, the following equation is also derived, where μ^2 is the square of the absolute value of the matrix element for the three-quantum transition, and where $T_2{}^{**}$ is a measure of the inverse observed linewidth:

$$\left(\frac{H_1{}^3S_s}{H_{1R}{}^3S}\right)^{2/3}=\frac{0.53}{(2\mu^2T_1T_2{}^{**}/\hbar^2)^{1/3}H_{1R}{}^{6/3}}+0.53(2\mu^2T_1T_2{}^{**}/\hbar^2)^{2/3}H_{1R}{}^{12/3}\left(\frac{H_1{}^2}{H_{1R}{}^2}\right)^3 \quad (3)$$

In Eqs. (2) and (3), $H_{1R}{}^2$ is an absolute reference power at the sample, the values of which are 9.7×10^{-4} and 7.5×10^{-3} G^2 respectively.

Results and Discussion

(i) Linewidth. Collision with any species perturbs the M_J levels by way of coupling between the orbital momentum and the electron spin state, and causes line broadening. For the O atom, the linewidth, ΔH_{msl}, is governed by the collision frequency; thus, ΔH_{msl} is proportional to the total pressure, by analogy with simple kinetic theory. The plots of ΔH_{msl} *vs.* the total pressure, shown in Fig. 1, all give

4) C. P. Poole, Jr., "Electron Spin Resonance," Interscience Publishers, Inc., New York, pp. 296—302.

5) H. Wahlquist, *J. Chem. Phys.*, **35**, 1708 (1961).

6) V. W. Hughes and J. S. Geiger, *Phys. Rev.*, **99**, 1842 (1955).

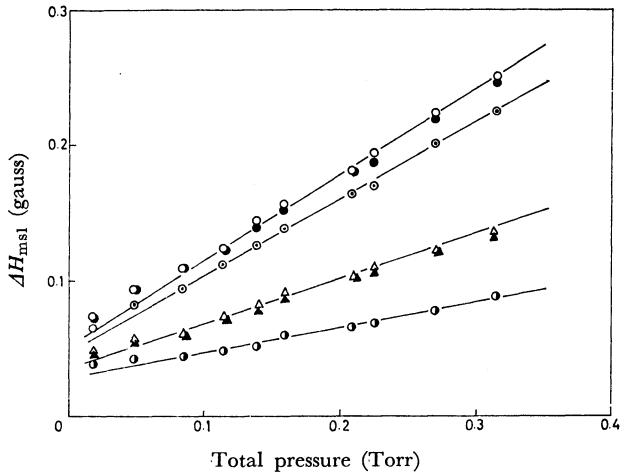

Fig. 1. Linewidths of O atom as a function of total pressure for the single-, two-, and three-quantum transitions.
⊙: $J=1$, $M_J=-1\rightarrow0$, ●: $J=2$, $M_J=-2\rightarrow-1$,
○: $J=2$, $M_J=-1\rightarrow0$, ▲: $J=2$, $M_J=-2\rightarrow0$,
△: $J=2$, $M_J=-1\rightarrow1$, ◑: $J=2$, $M_J=-2\rightarrow1$.

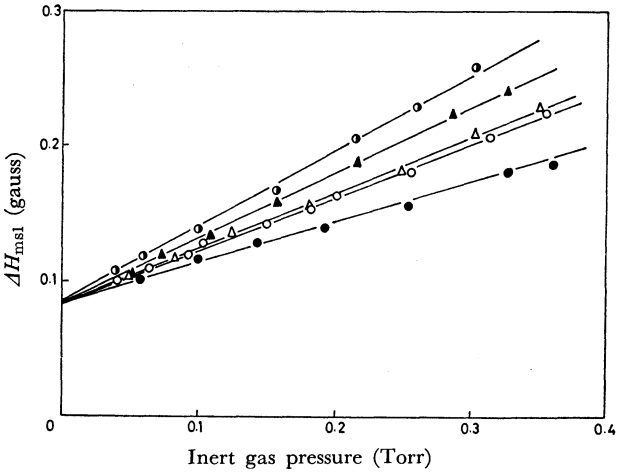

Fig. 2. Linewidths of O ($J=2$, $M_J=-1\rightarrow0$) atom as a function of inert gas pressure.
○: He, ●: Ne, △: Ar, ▲: Kr, ◑: Xe.

straight lines. For the $^3P_1$ state, the linewidths of the $M_J=-1\rightarrow0$ and $M_J=0\rightarrow1$ lines were equal to each other. For the $^3P_2$ state, the linewidths of the $M_J=-2\rightarrow-1$ and $M_J=1\rightarrow2$ lines were equal to each other, and the $M_J=-1\rightarrow0$ and $M_J=0\rightarrow1$ lines were also equal. Thus, the $M_J=-1\rightarrow0$ line of O($^3P_1$) and the $M_J=-2\rightarrow-1$ and $M_J=-1\rightarrow0$ lines of O($^3P_2$) were used for the width measurement, shown in Fig. 1. The cross sections for the line broadening were calculated for each line of the single-quantum transitions from the data in Fig. 1. The slopes of these linear plots give the values of the cross sections, $\sigma_{O(^3P_2)-O_2}=30.1$ Å^2 and $\sigma_{O(^3P_1)-O_2}=27.7$ Å^2, which are somewhat smaller than the value, $\sigma_{O-O_2}=37$ Å^2, obtained for the $M_J=-1\rightarrow0$ line of O($^3P_1$) by Westenberg and deHaas.[2]

The linewidths of the multiple-quantum transitions were noticeably smaller than those of the single-quantum transitions, as is to be expected from the theory of the multiple-quantum transitions.[6] The linewidths of the two- and three-quantum transitions are plotted against the total pressure, together with those of the single-quantum transitions, in Fig. 1. In the case of the two-quantum transition, the plots of the $M_J=-2\rightarrow0$ and $M_J=-1\rightarrow1$ lines are shown in Fig. 1, since the linewidths of the $M_J=-2\rightarrow0$ and $M_J=0\rightarrow2$ lines were equal to each other. In the case of the three-quantum transitions, the linewidths of the $M_J=-2\rightarrow1$ and $M_J=-1\rightarrow2$ lines were also equal; thus, the plots of the $M_J=-2\rightarrow1$ line are shown in Fig. 1. The apparent cross sections for the two- and three-quantum transitions are calculated from the slopes of the linear plots in Fig. 1 to be σ_{O-O_2} 14.6 Å^2 (two-quantum transition) and $\sigma_{O-O_2}=9.4$ Å^2 (three-quantum transition). These cross sections for the two- and three-quantum transitions are nearly 1/2 and 1/3 of those for the single-quantum transitions respectively. These relations coincide with that derived theoretically by Hughes and Geiger.[6]

In order to examine the pressure broadening, we added various inert gases, He, Ne, Ar, Kr, and Xe, as perturbers, keeping the partial pressure of oxygen constant at 0.048 Torr. Then, the variation in the linewidth of the $M_J=-1\rightarrow0$ line of O($^3P_2$) was measured; the plots of ΔH_{msl} *vs.* the pressure of inert gases are shown in Fig. 2. The slopes of these linear plots give the cross sections for the line-broadening collision. The values obtained are $\sigma_{O-He}=10.1$ Å^2, $\sigma_{O-Ne}=12.4$ Å^2, $\sigma_{O-Ar}=20.1$ Å^2, $\sigma_{O-Kr}=24.2$ Å^2, and $\sigma_{O-Xe}=28.2$ Å^2. The line-broadening cross sections obtained in this paper are larger than those obtained from the kinetic theory.

(ii) Relaxation Time. S-state atoms, which have no orbital angular momentum in the ground electronic configuration, have a long spin-lattice relaxation time, T_1, in the gaseous state. For N atoms, in the N_2 diluent, or for H atoms in the H_2 diluent, therefore, the saturation of ESR absorption by the atoms can be easily observed at a low microwave power, even at a high diluent pressure.[7] On the other hand, the observation of the saturation phenomena on O atoms in the $^3P_2$ and $^3P_1$ states needs a reduced oxygen diluent pressure and an increased microwave power.

By employing Eq. (1), the T_1 values for six single-quantum transitions of O($^3P_1$) and O($^3P_2$) are obtained from the saturation data. The plots of $(H_1/H_{1R}\cdot S_S/S)^{2/3}$ against the relative power (H_1^2/H_{1R}^2) at oxygen pressures from 0.02 to 0.3 Torr are shown in Fig. 3 for O($^3P_2$). The $(H_1/H_{1R}\cdot S_S/S)^{2/3}$ *vs.* (H_1^2/H_{1R}^2) plots for both O($^3P_1$) and O($^3P_2$) at a constant pressure of 0.139 Torr are also shown in Fig. 4 for the sake of comparison. These plots give linear lines with slopes of $0.53\ \{(2\mu^2T_1T_2/\hbar^2)^{2/3}H_{1R}^{4/3}\}$ and intercepts of $0.53/\{(2\mu^2T_1T_2/\hbar^2)^{1/3}H_{1R}^{2/3}\}$. It is possible to evaluate $T_1\cdot T_2$ from the value of either slopes or intercept. The values of $T_1\cdot T_2$ obtained in these two different ways almost coincided with each other. Since the lineshapes of the absorption spectra are

7) A. A. Westenberg and N. deHaas, *J. Chem. Phys.*, **40**, 3087 (1964).

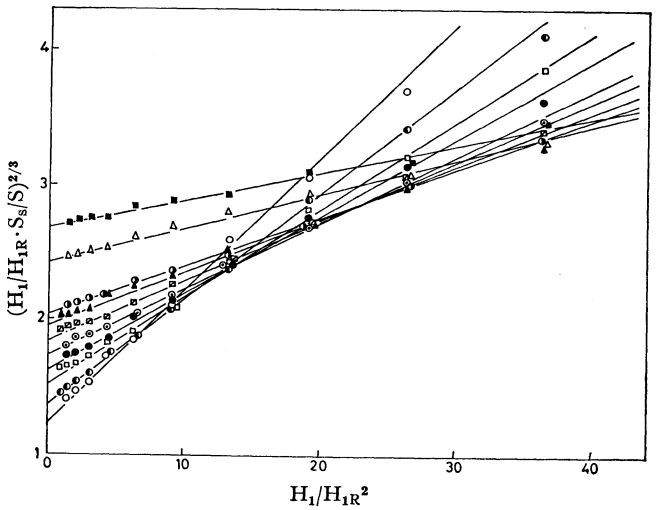

Fig. 3. Saturation data of O ($J=2$, $M_J=-1\rightarrow0$) atom. Data taken at the indicated total pressure in O_2 diluent. ○: 0.018, ◐: 0.048, □: 0.084, ●: 0.114, ⊙: 0.139, ◪: 0.159, ▲: 0.209, ◐: 0.225, △: 0.270, ■: 0.315 Torr.

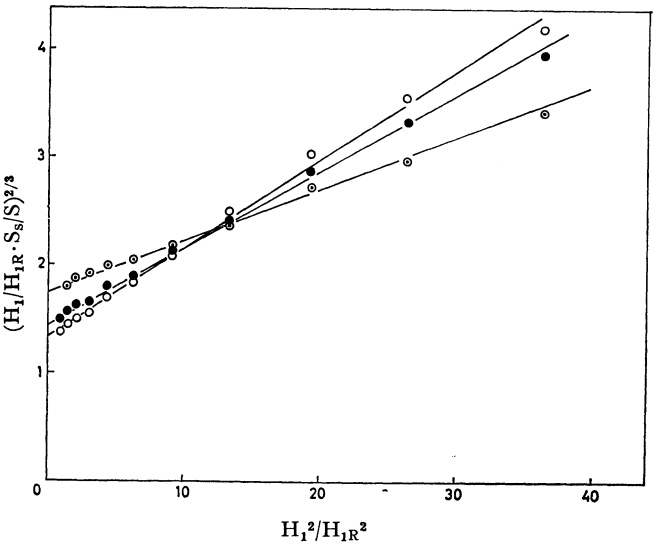

Fig. 4. Saturation data of the single-quantum transitions at total pressure of 0.139 Torr in O_2 diluent. ⊙: $J=1$, $M_J=-1\rightarrow0$, ●: $J=2$, $M_J=-2\rightarrow-1$, ○: $J=2$, $M_J=-1\rightarrow0$.

TABLE 1. EFFECT OF PRESSURE ON T_1 FOR O ATOM IN O_2 DILUENT

Total pressure (Torr)	$O(^3P_2)$ $M_J=-1\rightarrow0$ (μsec)	$O(^3P_2)$ $M_J=-2\rightarrow-1$ (μsec)	$O(^3P_2)$ $M_J=-1\rightarrow0$ (μsec)
0.018	1.15	1.06	1.03
0.048	1.02	0.85	0.81
0.084	0.87	0.81	0.76
0.114	0.84	0.77	0.74
0.139	0.76	0.72	0.65
0.159	0.71	0.66	0.63
0.209	0.60	0.55	0.52
0.225	0.58	0.51	0.48
0.270	0.45	0.42	0.40
0.315	0.37	0.38	0.35

Lorentzian at low modulation amplitudes and at a low microwave power, we can use the well-known relation $T_2=2/(\sqrt{3}\gamma\Delta H_{msl})$, where γ is $g\mu_B/\hbar$. Using this relation, we can calculate T_2, and then determine T_1 from the value of $T_1\cdot T_2$. These values are summarized in Table 1. In the case of inert-gas diluents, we calculated T_1 from the saturation data in the same manner. The values of T_1 thus obtained are summarized in Table 2. In order to obtain information on the relaxation mechanism, the plots of the reciprocal of T_1 *vs.* the total pressure for O_2 and inert-gas diluents are shown in Figs. 5 and 6 respectively. Especially, all of the plots of the inert-gas diluents were obtained from the saturation data on the $M_J=-2\rightarrow-1$ line of $O(^3P_2)$. Using the kinetic theory, the cross sections for the spin-lattice relaxation are calculated from the slopes of the linear portion in Figs. 5 and 6. The resulting cross sections are $\sigma_{O\text{-}He}=9.9$ Å^2, $\sigma_{O\text{-}Ne}=8.5$ Å^2, $\sigma_{O\text{-}Ar}=12.1$ Å^2, $\sigma_{O\text{-}Kr}=20.6$ Å^2, $\sigma_{O\text{-}Xe}=24.7$ Å^2, and $\sigma_{O\text{-}O_2}=33.3$ Å^2. Figure 7 shows plots of the cross sections against the atomic numbers of the inert gases, which serve as convenient indices. The figure also contains similar plots of the elastic scattering cross sections for collisions between electrons and the inert-gas atoms. The cross sections for the spin-lattice relaxation are about 6 times larger, but the sequence of the cross sections appears to be the same in both cases. A similar effect has been observed in the case of M_J mixing induced by potas-

TABLE 2. EFFECT OF INERT GAS ON T_1 FOR O ATOM ($M_J=-2\rightarrow-1$)

He (Torr)	T_1 (μsec)	Ne (Torr)	T_1 (μsec)	Ar (Torr)	T_1 (μsec)	Kr (Torr)	T_1 (μsec)	Xe (Torr)	T_1 (μsec)
0.041	0.88	0.058	0.86	0.048	0.86	0.050	0.84	0.039	0.85
0.064	0.86	0.100	0.83	0.082	0.84	0.073	0.82	0.059	0.81
0.093	0.85	0.143	0.81	0.124	0.81	0.108	0.77	0.099	0.73
0.103	0.81	0.193	0.78	0.181	0.75	0.157	0.68	0.157	0.63
0.150	0.73	0.254	0·70	0.248	0.65	0.216	0.59	0.216	0.53
0.182	0.68	0.327	0.63	0.302	0.61	0.286	0.47	0.260	0.44
0.201	0.66	0.360	0.55	0.350	0.49	0.329	0.45	0·303	0.41
0.256	0.54								
0.314	0.49								
0.355	0.44								

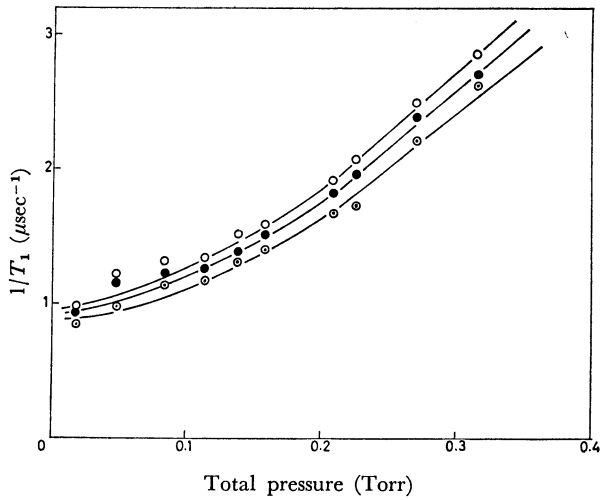

Fig. 5. Reciprocal of T_1 for the single-quantum transitions as a function of total pressure in O_2 diluent.
⊙: $J=1$, $M_J=-1\rightarrow 0$, ●: $J=2$, $M_J=-2\rightarrow -1$,
○: $J=2$, $M_J=-1\rightarrow 0$.

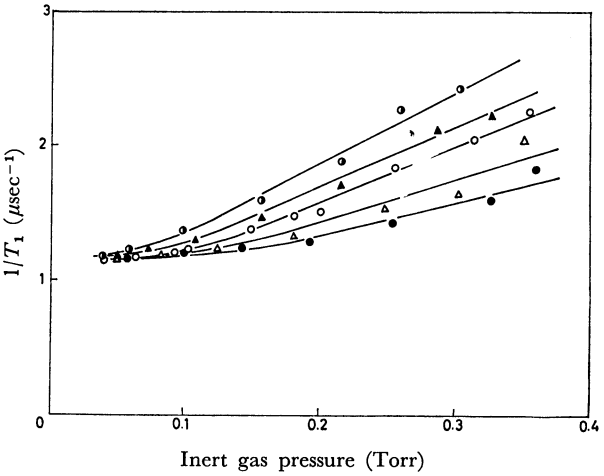

Fig. 6. Effects of added inert gases on T_1 for the single-quantum transitions ($J=2$, $M_J=-2\rightarrow -1$).
○: He, ●: Ne, △: Ar, ▲: Kr, ◑: Xe.

sium-inert gas atomic collisions.[8] It is probable between the orbital momentum and the electron-spin state by collision.

(iii) Multiple-quantum Transition. Observations of the multiple-quantum transitions for O atoms have been reported by Hughes and Geiger[6] and by McDonald.[3] Recently, Atherton and Cook[9] have discussed the lineshapes of the multiple-quantum transitions of $O(^3P_2)$, and Schindler and Tiedemann[10] have studied, both experimentally and theoretically, the change in the line intensities of the multiple-quantum transitions with the microwave power.

At a microwave power level of about 0.2 mW, only single-quantum transitions were detected. As the the power increased, the single-quantum transitions

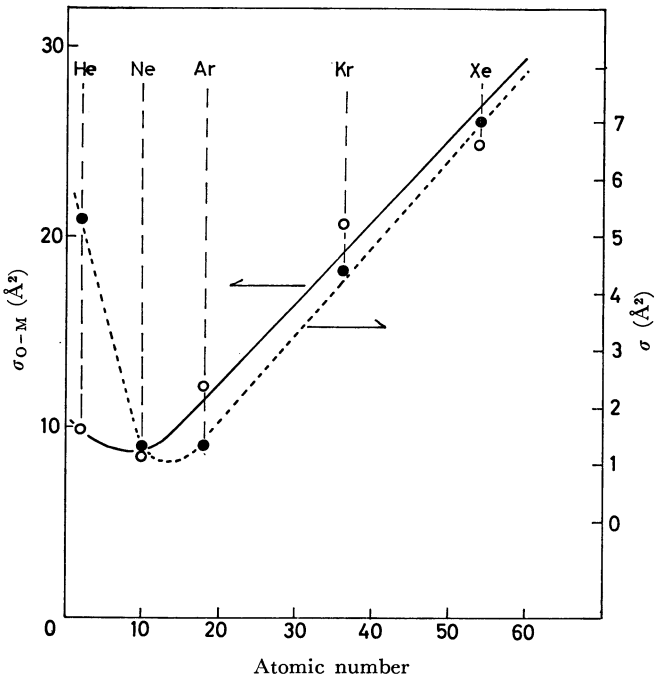

Fig. 7. For comparison of the cross sections (○) for the spin-lattice relaxation with the elastic scattering cross section (●).

showed saturation broadening, and, between each two lines of the four single-quantum transitions of $O(^3P_2)$, the two-quantum transitions appeared and increased in intensity. They became predominant in the spectrum at a microwave power level of about 2.5 mW. A further increase in power produced three-quantum transitions between the two-quantum transition lines, while the single-quantum transitions vanished in the noise level and the two-quantum transitions showed a saturation broadening. At about 20 mW, the three-quantum transitions gave the strongest lines in the spectrum. Finally, between the three-quantum transition lines, the four-quantum transition could be detected at about 100 mW. Thus, by virtue of the different saturation properties of the various transitions, all the possible multiple-quantum transitions for $O(^3P_2)$ can be observed. It is interesting to measure the spin-lattice relaxation time, T_1, of the multiple-quantum transitions, since the saturation property is closely related with the spin-lattice relaxation phenomena.

Extending the treatment employed to measure T_1 for the single-quantum transitions, we tried to obtain for the multiple-quantum transitions from Eqs. (2) and (3), which were derived theoretically. The plots of $(H_1^2/H_{1R}^2\cdot S_S/S)^{2/3}$ *vs.* $(H_1^2/H_{1R}^2)^2$ for the two-quantum transitions, and those of $(H_1^3/H_{1R}^3\cdot S_S/S)^{2/3}$ *vs.* (H_1^2/H_{1R}^3) for the three-quantum transitions, are shown in Figs. 8 and 9 respectively. Using Eqs. (2) and (3), we can obtain $T_1\cdot T_2^*$ and $T_1\cdot T_2^{**}$ from the slopes of these linear plots in Figs. 8 and 9. We can determine T_2^* and T_2^{**} from the observed linewidths of the two- and three-quantum transition lines, and then calculate T_1 from the values of $T_1\cdot T_2^*$ and $T_1\cdot T_2^{**}$. The values of T_1 obtained for the two- and three-

8) W. Berdowski and L. Krause, *Phys. Rev.*, **165**, 158 (1968).
9) N. M. Atherton and Irene P. Cook, *Mol. Phys.*, **19**, 417 (1970).
10) P. Tiedemann and R. N. Schindler, *J. Chem. Phys.*, **54**, 797 (1971).

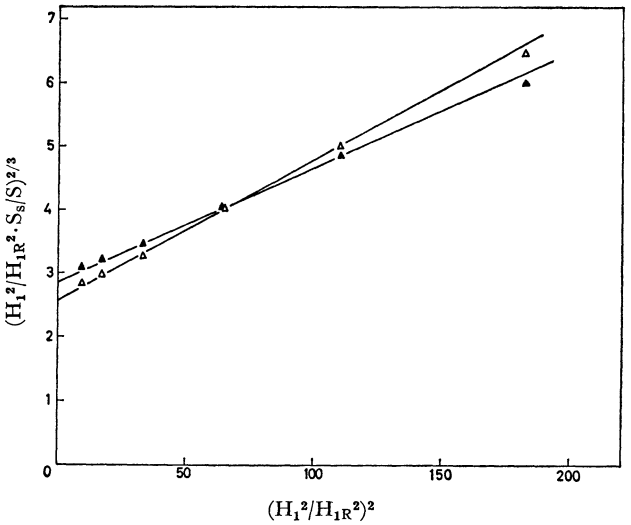

Fig. 8. Saturation data of the two-quantum transitions at total pressure of 0.139 Torr in O_2 diluent.
▲: $J=2$, $M_J=-2\rightarrow0$, △: $J=2$, $M_J=-1\rightarrow1$.

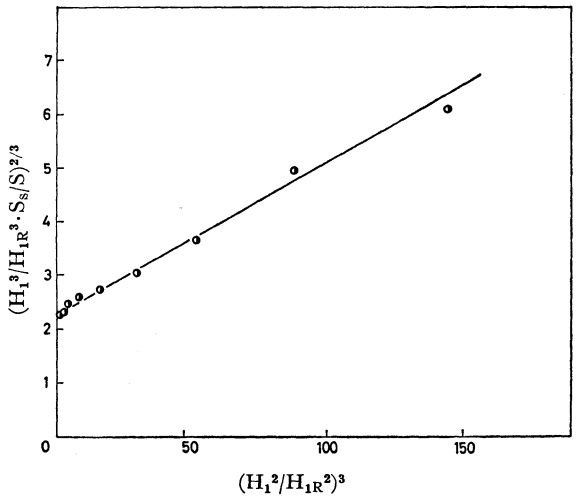

Fig. 9. Saturation data of the three-quantum transitions ($J=2$, $M=-2\rightarrow1$) at total pressure of 0.139 Torr in O_2 diluent.

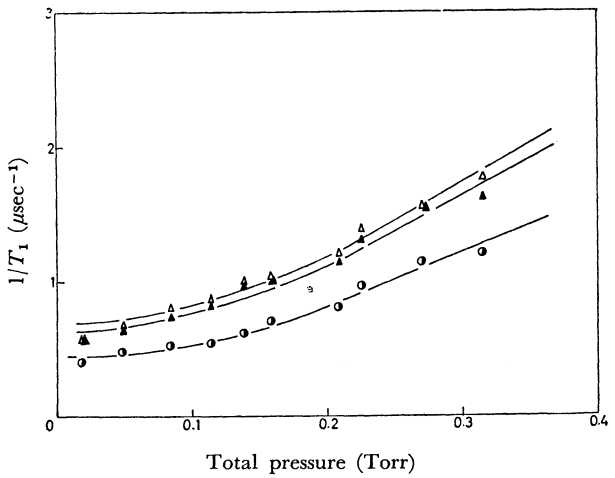

Fig. 10. Reciprocal of T_1 for the two- and three-quantum transitions as a function of total pressure in O_2 diluent.
▲: $J=2$, $M_J=-2\rightarrow0$, △: $J=2$, $M_J=-1\rightarrow1$,
◐: $J=2$, $M_J=-2\rightarrow1$.

TABLE 3. EFFECTS OF PRESSURE OF T_1 FOR THE TWO- AND THREE-QUANTUM TRANSITION IN O_2 DILUENT

Total pressure (Torr)	Two-quantum transition $M_J=-2\rightarrow0$ (μsec)	Two-quantum transition $M_J=-1\rightarrow1$ (μsec)	Three-quantum transition $M_J=-2\rightarrow1$ (μsec)
0.018	1.75	1.74	2.44
0.048	1.62	1.55	2.05
0.084	1.27	1.24	1.89
0.114	1.21	1.16	1.83
0.139	1.02	0.99	1.65
0.159	0.97	0.95	1.40
0.209	0.88	0.84	1.26
0.225	0.77	0.73	1.05
0.270	0.65	0.65	0.89
0.315	0.62	0.57	0.84

quantum transitions are summarized in Table 3. It is found that the values of T_1 for the single-, two-, and three-quantum transitions decrease in that order. In order to examine the relaxation mechanism, we have plotted $1/T_1$ *vs.* the pressure in Fig. 10. The plots are linear except at low pressures, and the dependence of $1/T_1$ on the pressure is in the same sequence for the two- and three-quantum transitions as for the single-quantum transition. From the data in Fig. 10, the values of the apparent cross sections for the spin-lattice relaxation are found to be $\sigma_{O-O_2}=18.0$ Å^2 (two-quantum transition) and $\sigma_{O-O_2}=14.0$ Å^2 (three-quantum transition), which are smaller than $\sigma_{O-O_2}=33.3$ Å^2 of the single-quantum transition for $O(^3P_2)$.

In order to examine the relaxation mechanism in Zeeman sublevels, we derived the relationship between the transition probabilities induced by collisional interaction and the spin-lattice relaxation time (*cf.* the Appendix). From these relationships, the following results can be expected. In the case of the single-quantum transition, the T_1 values of the $M_J=-2\rightarrow-1$ and $M_J=1\rightarrow2$ lines are equal to each other, while those the $M_J=-1\rightarrow0$ and $M_J=0\rightarrow1$ lines are also equal. In addition, the T_1 value of the former pair is smaller than that of the latter. In the case of the two-quantum transition, the T_1 values of the $M_J=-2\rightarrow0$ and $M_J=0\rightarrow2$ lines are equal to each other, and T_1 of this pair has a smaller value than that of the $M_J=-1\rightarrow1$ line. In the case of the three-quantum transition, the T_1 values of the $M_J=-2\rightarrow1$ and $M_J=-1\rightarrow2$ lines are also equal. These results, expected from the Appendix, are in fair qualitative agreement with the experimental results (Tables 1 and 3). As the Appendix shows, the four transition probabilities can be estimated using the values of T_1 for the single-, two-, and three-quantum transitions obtained experimentally. Under these experimental conditions, the $W_1 \gg W_2 > W_3 > W_4$ relation can be expected. Assuming that the values of W_3 and W_4 are negligibly small, the values of W_1 and W_2 can be calculated from the values of T_1 obtained in the pressure range from about 0.2 to 0.3 Torr by the method of least-squares. The average value of W_2/W_1 is 0.0339

in this pressure range, which shows roughtly that the relaxation may be carried out step-by-step; *i.e.* the single-quantum relaxation mainly occurs even in the case of the miltiple-quantum transition.

Appendix

The corresponding probabilities of the $\Delta M_J=\pm1$, ±2, ±3, and ±4 transitions between five Zeeman sublevels ($M_J=-2$, -1, 0, 1, 2) of the $^3P_2$ states induced by the collisions O of atoms with oxygen molecules are $W_{\pm1}$, $W_{\pm2}$, $W_{\pm3}$, and $W_{\pm4}$ respectively, assuming that the sublevels are approximately equally spaced. We suppose that the populations of the substates are N_{-2}, N_{-1}, N_0, N_1, and N_2. In a thermal equilibrium, the steady-state populations obey Boltzmann's law; this requires that the probabilities for transitions up and down be in the ratios of:

$$\begin{aligned}\frac{W_{+1}}{W_{-1}} &= \exp(g\beta H/\boldsymbol{k}T)\\ \frac{W_{+2}}{W_{-2}} &= \exp(2g\beta H/\boldsymbol{k}T)\\ \frac{W_{+3}}{W_{-3}} &= \exp(3g\beta H/\boldsymbol{k}T)\\ \frac{W_{+4}}{W_{-4}} &= \exp(4g\beta H/\boldsymbol{k}T)\end{aligned} \tag{A-1}$$

Since $g\beta H \ll \boldsymbol{k}T$, we can satisfy these conditions by taking:

$$\begin{aligned}W_{\pm1} &= W_1\left(1 \pm \frac{1}{2}\frac{g\beta H}{\boldsymbol{k}T}\right)\\ W_{\pm2} &= W_2\left(1 \pm \frac{g\beta H}{\boldsymbol{k}T}\right)\\ W_{\pm3} &= W_3\left(1 \pm \frac{3}{2}\frac{g\beta H}{\boldsymbol{k}T}\right)\\ W_{\pm4} &= W_4\left(1 \pm \frac{2g\beta H}{\boldsymbol{k}T}\right)\end{aligned} \tag{A-2}$$

By way of example, we will try to obtain the relationship between the transition probabilities and T_1 for the two-quantum transition ($M_J=-1\rightarrow1$). We consider the initial conditions:

$$\begin{aligned}&N_{-2} = N+2n_0,\ N_{-1} = N+n,\ N_0 = N,\\ &N_1 = N-n,\ N_2 = -2n_0\end{aligned} \tag{A-3}$$

with a small n value, where n_0 is the equilibrium value of n. The time evolution of n obeys the following differential equations:

$$\begin{aligned}\frac{dn}{dt} &= -(W_{+1}+W_{-3}+W_{-2}+W_{-1})(N+n)\\ &\quad +W_{+2}(N-n)+W_{+1}N+W_{+3}(N-2n_0)\\ &\quad +W_{-1}(N+2n_0)\\ -\frac{dn}{dt} &= -(W_{+3}+W_{+2}+W_{+1}+W_{-1})(N-n)\\ &\quad +W_{-2}(N+n)+W_{-1}N+W_{+1}(N-2n_0)\\ &\quad +W_{-3}(N+2n_0)\end{aligned} \tag{A-4}$$

Substituting the probabilities from (A-2), we find that:

$$\frac{dn}{dt} = (2W_1+2W_2+W_3)(n_0-n). \tag{A-5}$$

The spin-lattice relaxation time is:

$$\frac{1}{T_1} = (2W_1+2W_2+W_3). \tag{A-6}$$

In the same manner, we can get the following relation between the transition probabilities and T_1 for the single-, two-, three-, and four-quantum transitions.

(i) single-quantum transition

$$M_J = -2\rightarrow-1 \quad \frac{1}{T_1} = \frac{1}{2}(5W_1+2W_2+2W_3+W_4)$$

$$M_J = -1\rightarrow0 \quad \frac{1}{T_1} = \frac{1}{2}(6W_1+3W_2+W_3)$$

$$M_J = 0\rightarrow1 \quad \frac{1}{T_1} = \frac{1}{2}(6W_1+3W_2+W_3)$$

$$M_J = 1\rightarrow2 \quad \frac{1}{T_1} = \frac{1}{2}(5W_1+2W_2+2W_3+W_4)$$

(ii) two-quantum transition

$$M_J = -2\rightarrow0 \quad \frac{1}{T_1} = \frac{1}{2}(3W_1+5W_2+W_3+W_4)$$

$$M_J = -1\rightarrow1 \quad \frac{1}{T_1} = (2W_1+2W_2+W_3)$$

$$M_J = 0\rightarrow2 \quad \frac{1}{T_1} = \frac{1}{2}(3W_1+5W_2+W_3+W_4)$$

(iii) three-quantum transition

$$M_J = -2\rightarrow1 \quad \frac{1}{T_1} = \frac{1}{2}(3W_1+2W_2+4W_3+W_4)$$

$$M_J = -1\rightarrow2 \quad \frac{1}{T_1} = \frac{1}{2}(3W_1+2W_2+4W_3+W_4)$$

(iv) four-quantum transition

$$M_J = -2\rightarrow2 \quad \frac{1}{T_1} = (W_1+W_2+W_3+2W_4)$$